Teriflunomide Promotes Blood-Brain Barrier Integrity by Upregulating Claudin-1 via the Wnt/β-catenin Signaling Pathway in Multiple Sclerosis

Zhao Yipeng
The Third Affiliated Hospital of Sun Yat-sen University
Chen Chen
The Third Affiliated Hospital of Sun Yat-sen University
Xiao Xiuqing
Fuwai Hospital Chinese Academy of Medical Sciences
Fang Ling
The Third Affiliated Hospital of Sun Yat-sen University
Chang Yanyu
The Third Affiliated Hospital of Sun Yat-sen University
Cheng Xi
The Third Affiliated Hospital of Sun Yat-sen University
Peng Fuhua
The Third Affiliated Hospital of Sun Yat-sen University
Wang Jingqi
The Third Affiliated Hospital of Sun Yat-sen University
Shen Shishi
The Third Affiliated Hospital of Sun Yat-sen University
Wu Shilin
The Third Affiliated Hospital of Sun Yat-sen University
Cai Wei
The Third Affiliated Hospital of Sun Yat-sen University
Qiu Wei (qiuwei@mail.sysu.edu.cn)
The Third Affiliated Hospital of Sun Yat-sen University

Research Article

Keywords: Multiple sclerosis, Blood-brain barrier, Teriflunomide, Claudin-1, Wnt signaling pathway

Posted Date: September 2nd, 2022

DOI: https://doi.org/10.21203/rs.3.rs-2004378/v1

Abstract

Background The blood-brain barrier (BBB) and tight junction (TJ) proteins maintain the homeostasis of the central nervous system (CNS). The dysfunction of BBB allows peripheral T cells infiltration into CNS and contributes to the pathophysiology of multiple sclerosis (MS). Teriflunomide is an approved drug for the treatment of MS by suppressing lymphocytes proliferation. However, whether teriflunomide has a protective effect on BBB in MS is not understood.

Methods The analysis of MS patient samples, experiment autoimmune encephalomyelitis (EAE) rat model and BBB cell models were performed to evaluate the function of teriflunomide on BBB. The promotion of teriflunomide on TJ proteins was assessed by qPCR, western blotting, immunofluorescence, transendothelial electrical resistance (TEER) measurement and NaF transmittance. After RNA sequencing, downstream signaling pathway were screened and verified using agonists, inhibitors and gene knockdown. The protective effect of teriflunomide-regulated pathway on BBB was further examined in EAE model.

Results Teriflunomide restored the injured BBB in EAE model. Furthermore, teriflunomide treatment over six months improved BBB permeability and reduced peripheral leakage of CNS proteins in MS patients. Teriflunomide increased human brain microvascular endothelial cells (HBMECs) viability and promoted BBB integrity in an **in vitro** cell model. The TJ protein claudin-1 was upregulated by teriflunomide and responsible for the protective effect on BBB. Furthermore, RNA sequencing revealed that the Wnt signaling pathway was affected by teriflunomide. The activation of Wnt signaling pathway increased claudin-1 expression and reduced BBB damage in cell model and EAE rats.

Conclusion Our study demonstrated that teriflunomide upregulated the expression of the tight junction protein claudin-1 in endothelial cells, and promoted the integrity of BBB through Wnt signaling pathway.

Introduction

Multiple sclerosis (MS) is an autoimmune disease of the central nervous system (CNS) characterized by autoreactive lymphocytes passing through the impaired blood–brain barrier (BBB), causing demyelination and neuro-axonal degeneration[1, 2]. Current therapeutic strategies mainly focus on the suppression of autoimmune T and B cells to ameliorate intracranial demyelinating lesions and modify the overall disease course[3]. For example, disease-modifying therapies (DMTs) can effectively reduce inflammatory levels and thus improve MS progression[4, 5]. However, most treatments have no effect on the injured BBB. Once the treatment is stopped, the burst of inflammatory cells will cross the BBB and cause more CNS damage[6].

The BBB maintains the homeostasis of the CNS by preventing the entry of peripheral cells and molecules[7]. Tight junctions (TJs) in endothelial cells are necessary for the formation of the impermeable barrier. TJ proteins are composed of proteins complexes, including claudin, occludin and zonula occludens (ZO)[8]. BBB dysfunction contributes the pathophysiology of MS. At the onset of MS, T

cells produce many inflammatory cytokines and disrupt the TJ proteins between endothelial cells, resulting in an enlarged gap in the BBB for infiltration into the CNS[9, 10].

Teriflunomide, an approved disease modifying treatment (DMT) drug for the treatment of relapsing-remitting MS (RRMS), is a cytostatic inhibitor of dihydroorotate dehydrogenase (DHODH) used to suppress lymphocyte proliferation[11, 12]. However, teriflunomide has been reported to modulate multiple signaling pathways, such as the store-operated calcium entry (SOCE), MAPK, and the p53, suggesting that teriflunomide is involved in other celluar processes, such as cell cycle regulation, differentiation and apoptosis[13-15]. However, whether teriflunomide protects the BBB in MS is not fully understood.

In this study, we found that teriflunomide restored BBB damage in MS patients and an experimental autoimmune encephalomyelitis (EAE) model. Based on these findings, we hypothesized that teriflunomide had a protective effect on the BBB. As a result, teriflunomide increased endothelial cell viability. Furthermore, teriflunomide promoted the expression of the TJ protein claudin-1 (encoded by the *CLDN1* gene) to enhance the integrity of the BBB model *in vitro*. RNA-sequence analysis further showed that the Wnt signaling pathway was involved in the regulation of claudin-1 and BBB impermeability by teriflunomide. Wnt agonists could improve clinical scores and alleviate disease progression in the EAE model by promoting claudin-1 expression. Our study demonstrated that teriflunomide had a protective effect on the BBB by upregulating claudin-1 expression on endothelial cells in MS pathogenesis.

Methods

Induction of EAE model

Female Lewis rats at 6-8 weeks of age were purchased from Beijing Vital River Laboratory Animal Technology Co., Ltd (Beijing, China). The antigen emulsion was prepared from an emulsion of guinea pig spinal cord white matter homogenates in phosphate-buffered saline (PBS, 50% w/v) mixed with an equal volume of complete Freund's adjuvant (Sigma-Aldrich) supplemented with 4 mg/mL Mycobacterium tuberculosis. Each rat was immunized by subcutaneous injection of antigen emulsion at a dose of 0.75 ml/kg into its footpad, followed by an auxiliary injection of 8 μg/kg diluted in 0.5 mL pertussis toxin (List Biological Laboratories) in the dorsum of the foot. The second immunization was administered 7 days after the first immunization. Clinical signs of EAE were monitored daily. According to different groups, animals were orally treated with teriflunomide (10 mg/kg) diluted in the Tween 80 or Wnt agnonist R-spondin1 (1mg/kg) or Tween 80 once daily.

After immunization, the rats were observed in a double-blind manner every day and given clinical scores with the following criteria: 0, no clinical signs; 0.5, partial loss of tail tone; 1, affected tail tonus; 2, paresis of hind legs; 3, complete paralysis of the hind legs; 4, complete hind leg paralysis and foreleg paresis; and 5, death due to EAE. These criteria were established and modified according to previous clinical scale systems.

BBB permeability *in vivo*

For analysis of BBB permeability in the EAE model, 2% Evans blue in PBS were injected intravenously into the tail vein (4mg/kg) of rats. 24 h after injection, rats were perfused with PBS, and the brain and spinal cord were removed. Tissues were homogenized in in 5 ml of formamide and were maintained at room temperature for 48 h. Samples were centrifuged at 14,500g for 30 min, and the supernatant was removed for analysis. The absorbance of the supernatant at 630 nm was measured with a microplate reader (BioTek, Winooski, USA).

NFLs detection

Serum samples were separated at the peak of EAE. The levels of NFLs in each sample were measured by the scanning microplate reader (BioTek, Winooski, USA) using the Bradford method according to the manufacturer's instructions (Simoa NF-Light Advantage Kit, 103186).

Clinical analysis

For the serum samples, we included all RRMS patients referred for MRI by the MS clinic at our hospital. Inclusion criteria were: (1) an established diagnosis of MS, (2) clinical indication for treatment with definite drug use, (3) age=15 to 50 years and (4) disease duration less than 15years. For DCE-MRI, on a voluntary basis, we included 11 patients with exclusion criteria: (1) other concurring disease and (2) contraindication to MRI scan or MRI contrast agent.

DCE-MRI was performed on a 3T magnetic resonance unit (Verio, Siemens AG, Erlangen, Germany) using a 20-element phased-array head coil. Two pre-contrast T1-weighted (flip angle 2° and 15°, TR/TE 4.09/1.42 ms, 3.0 mm slice thickness, FOV 230 mm * 230 mm, matrix 192 * 192 * 77) images were acquired. After the pre-contrast scan, 60 dynamic contrast-enhanced T1-Weighted (flip angle 15°, TR/TE 5.08/1.8 ms, 3.0 mm slice thickness, FOV 230 mm * 230 mm, matrix 192 * 192 * 77) images were obtained. Then, a bolus dose of 0.1 mmol/kg of gadolinium-based contrast agent (Bayer AG, Leverkusen, Germany) was injected intravenously via the elbow at 3 mL/s with a power injector, followed by 20 mL of normal saline for irrigation.

The DCE-MRI processing was dealt with the commercial software tool (Tissue 4D, Syngo.via, Siemens Healthcare) including motion correction, alignment, and processing. The concentration curve of the volume of interest was generated according to the Tofts model. A population-based arterial input function (AIF) was used and set to "fast", "intermediate", or "slow" model with the minimum of chi-square parameter. Regions of interest (ROIs) were drawn on lesions to each of permeability maps (Ktrans, Kep, Ve, and iAUC). For each subject, we used the median value of permeability to exclude effects of possible outliers.

Cell culture and treatment

The human brain microvascular endothelial cells (HBMECs) was purchased from BeNa Culture Collection Co. Ltd (Beijing, China) and cultured with endothelial cell medium (ECM). The different concentrations of teriflunomdie (MCE, HY-15405), fingolimod (MCE, HY-11063), dimethyl fumarate (MCE, HY-17363) and

mannitol (Aladdin, M119324) were added in the medium for 48 h to observe the effects on HBMECs viabilities. 10 ng/ml TNF (Proteintech, HZ-1014) and 5 ng/ml IFN-γ (Proteintech, HZ-1301) were used for inflammatory stimulation. Wnt signal pathway modulator LGK974 (1 nM, MCE, HY-17545), IWR-1 (10 μM, MCE, HY-12238), R-spondin1 (10 ng/ml, Proteintech, HZ-1328) and SKL2001 (20 μM, MCE, HY-101085) were added in the medium for 48 h to observe the regulation of Wnt signaling on HBMECs. SiRNA of *CLDN1* or *CTNB* (RIBOBIO) was transfected into HBMECs with INTERFERin (DAKAWE).

Cytotoxicity assay

Cell viabilities were measured with CCK-8 according to the manufacturer's instructions. Briefly, 5 μl of CCK-8 reagent was added into each well and incubated for 1-4 hours. The absorbances at 450 nm were measured using the scanning microplate reader (BioTek, Winooski, USA).

BBB permeability *in vitro*

The HBMECs were cultured in polyester transwell (1×10^5 cells per well). When the cells reached confluence, the formed monolayer was used to mimic the BBB morphology and activity *in vitro*. We used a Millicell-ERS volt-ohmmeter (Millipore, Burlington, USA) to monitor the integrity of the monolayer. The NaF solution was added to the upper layer of the transwell and the lower layer was measured 1 hour later using the scanning microplate reader (BioTek, Winooski, USA).

Quantitative PCR

Total RNA was isolated using TRIzol reagent according to the manufacture's protocols. Then, cDNA was synthesized using a SuperScript VILO cDNA Synthesis Kit. Quantitative PCR was performed using the StepOnePlus Real-Time PCR System (Life Technologies, New York, USA). The levels of gene expression were normalized to GAPDH. The specific primers (synthesized by GENEWIZ, Suzhou, China) were used as following: *TJP1* (forward: AAAGGCGGATGGTGCTACAA, reverse: CGCCTTCTGTGTCTGTGTCT), *TJP2* (forward: TGAAGACA CGGACGGTGAAG, reverse: GTCCACGAGAGTGCAAGGAA), *TJP3* (forward: TGTGGCCTCATGCCCATCTT, reverse: GATCGCAATGCCA AAGCCC), *OCLN* (forward: AGCAGCGGTGGTAACTTTGA, reverse: CCTCCAGCTCATCACAGGAC), *JAM1* (forward: GGCGGCTGTTGTG TCAGTG, reverse: CGAGTAGGCACAGGACAACTT), *JAM2* (forward: AGGCCTATGGGTTTTCTGCC, reverse: CAAAGGAGACACTCCGA CCC), *JAM2* (forward: AGGCCTATGGGTTTTCTGCC, reverse: CAA AGGAGACACTCCGACCC), *JAM3* (forward: GCCCCTCAGCAACCC TC, reverse: TACCACTGGGGTTCGATTGC), *CLDN1* (forward: CTGT CATTGGGGGTGCGATA, reverse: CTGGCATTGACTGGGGTCAT), *CLDN3* (forward: TCGGCCAACACCATTATCCG, reverse: CCGTG TACTTCTTCTCGCGT), *CLDN5* (forward: TGTCGCAGAAGTACGAG CTG, reverse: TCTTCTTGTCGTAGTCGCCG), *CLDN12* (forward: TGT ACCTCGCTGGGAACG, reverse: ATCTGAGCCTGCTTCTCACAC), *beta-actin* (forward: TTCCTTCCTGGGCATGGAGT, reverse: AATGC CAGGGTACATGGTGG).

Western blot

The cultured cells were lysed on ice by RIPA lysates. Protein concentrations were determined with a BCA Protein Quantitation Kit. A total of 10-30 μg protein was loaded in each lane and was separated by 10% SDS-PAGE. After separation, the proteins were transferred to PVDF membranes. The membranes were blocked with 5% defatted milk powder for 1 h. Blots were incubated overnight with the primary antibodies as follows: ZO-1 (1:500, Abcam, ab96587), occludin (1:500, Abcam, ab235986), claudin-5 (1:1000, Abbkine, abp50990), claudin-1 (1:500, CST signaling, 13995S) and β-catenin (1:500, CST signaling, 9587T). The β-actin (1:3000, Proteintech, 66009-1-Ig) was used as a control. Then horseradish peroxidase (HRP)-conjugated secondary antibody were incubated with corresponding primary antibody blots for 1h. Blots were visualized using the ECL western blotting substrate and recorded by the gel imager (Bio-Rad, Hercules, USA).

Immunohistochemistry

For monochromatic immunofluorescence, the cells were cultured in confocal dishes. After fixed with 4% paraformaldehyde for 15 min, triton X-100 (1%) were incubated with cells for 15 min to help the antibody permeating the cell membrane. Then, cells were blocked with 1% of goat serum for 1 h and incubated with antibodies at 4°C overnight. After washed with PBS for three times, cells were incubated with fluorochrome conjugated antibodies for 1 h. Next, DAPI was added for nuclei staining. The images were collected by confocal microscopy (Zeiss, Oberkochen, Germany) and analyzed by Image J software.

For polychromatic immunofluorescence, the sections were incubated with single primary antibody followed by corresponding fluorochrome conjugated second antibody. After staining, the sections were washed and stained for the next indicator. Primary antibodies were used as following: ZO-1 (1:100, Abcam, ab96587), occludin (1:100, Abcam, ab235986), claudin-5 (1:100, Abbkine, abp50990), claudin-1 (1:100, CST signaling, 13995S), β-catenin (1:100, CST signaling, 9587T) and Wnt2b (1:100, invitrogen, MA5-42480).

RNA sequencing

Total RNA of cultured HBMECs was isolated using TRIzol reagent (Invitrogen) according to the manufacturer's protocol. The RNA was qualified and quantified using a Nano Drop and Agilent 2100 bioanalyzer (Thermo Fisher Scientific, USA). The strand-specific cDNA libraries were generated and amplified with phi29 to make DNA nanoball (DNB) which had more than 300 copies of one molecular, DNBs were loaded into the patterned nanoarray and single end 50 bases reads were generated on BGIseq500 platform.

The sequencing data was filtered with SOAPnuke by (1) Removing reads containing sequencing adapter; (2) Removing reads whose low-quality base ratio (base quality less than or equal to 5) is more than 20%; (3) Removing reads whose unknown base ratio is more than 5%, afterwards clean reads were obtained and stored in FASTQ format. The clean reads were mapped to the reference genome using HISAT2. Bowtie2 was applied to align the clean reads to the reference coding gene set, then expression level of gene was calculated by RSEM. The heatmap was drawn by PHEATMAP according to the gene expression

in different samples. Essentially, differential expression analysis was performed using the DESeq2 with Q value ≤ 0.05. To take insight to the change of phenotype, GO and KEGG enrichment analysis of annotated different expressed gene was performed by Phyper based on Hypergeometric test. The significant levels of terms and pathways were corrected by Q value with a rigorous threshold (Q value ≤ 0.05) by Bonferroni.

Luxol fast blue (LFB) staining

After the experiments, anesthetized rats were intracardially perfused with PBS, followed by 4% paraformaldehyde in PBS. The rats were euthanized, and the lumbar spinal cords were removed and immersed for 48 hours in 4% paraformaldehyde for fixation. 4 μm thick transverse sections taken from embedded blocks of spinal cord were deparaffinized and stained with LFB to assess demyelination.

Statistics

Data are presented as the mean ± s.e.m. of at the least three independent experiments. For experiments with two groups, Student's t test was used for statistical analysis. For experiments with multiple comparisons, significance was determined using ANOVA with Newman-Keuls test. The clinical scores curves were statistically analyzed by the generalized equation. *p 0.05, **p 0.01, ***p 0.001.

Results

Teriflunomide restored BBB integrity in an EAE model and MS patients

To study the protective effect of teriflunomide on the BBB, we induced EAE in a rat model and orally administered teriflunomide. As shown in Fig. 1A, the preventive and therapeutic teriflunomide treatment significantly decreased the clinical score of EAE rats. Then, Evans blue was peripherally injected at the peak of EAE and infiltrations into the CNS was measured to evaluate BBB integrity [16]. After injection, the spinal cords of EAE rats exhibited the diffusion of Evans blue dye, suggesting breakdown of the BBB after EAE induction. Teriflunomide effectively decreased the concentrations of Evans blue in the CNS (Fig. 1B, C). In addition, the leakage of neurofilament light chains (NFLs) into the serum, which is a biomarker of neuronal damage in MS and is associated with loss of BBB integrity, was also reduced by teriflunomide treatment (Figure 1D)[17, 18]. These results demonstrate a protective effect of teriflunomide on the BBB of EAE rats.

TJ proteins form the TJ structure of the BBB and maintain its impermeability. We examined common TJ protein markers of the BBB to evaluate whether teriflunomide affected these proteins. ZO-1 binds to the actin cytoskeleton through its C-terminus, serving as a bridge between transmembrane proteins and the cytoskeleton. This interaction is important for the stability and function of TJs[19]. Claudin-5 is a hallmark of the BBB and plays an essential role in the earliest stage of CNS angiogenesis[20]. Occludin is the first identified membrane protein within TJs and the truncation of both the C-terminus and N-terminus of occludin decreases transendothelial electrical resistance (TEER), suggesting a key role of occludin in

the barrier function of TJs[21]. The expression of ZO-1, claudin-5, and occludin were decreased in EAE rats, indicating serious destruction of the BBB after EAE induction (Fig. 1E-H). Therapeutic teriflunomide treatment restored the expression of claudin-5, suggesting that teriflunomide had a role in claudin-5 regulation (Fig. 1E, G). In addition, the levels of occludin in the preventive teriflunomide group was higher than in the EAE group (Fig. 1E, H). This difference might be due to the prophylactic treatment that inhibited inflammatory cells and prevented the loss of TJ proteins.

In addition, we also verified the protective role of teriflunomide in MS patients. First, the concentration of NFLs in the MS patients was higher than that observed in healthy controls (Fig. 2A), suggesting degradation of the BBB during MS progression. Treatments can effectively reduce NFL leakage, and we found that teriflunomide was more effective than other DMT drugs (fingolimod and dimethyl fumarate).

Furthermore, dynamic contrast enhanced magnetic resonance imaging (DCE-MRI) was used to assess the integrity of the BBB in MS volunteers (Table.1)[22]. The results showed that the values of the volume transfer constant (K^{trans}) and Kep (indicated rate transfer coefficient) were decreased after teriflunomide treatment for over 6 months (Fig. 2B, C). The volume fraction of extravascular extracellular space (Ve) was not different between the groups (Fig. 2D). These results indicated that teriflunomide ameliorated the BBB injuries in MS patients. In addition, we collected the images from one patient after treatment with teriflunomide for 3 months and 6 months (Fig. 2E, F). Six months of teriflunomide treatment greatly improved BBB damage compared to three months. These clinical studies showed that teriflunomide promoted the restoration of the BBB in MS patients.

Teriflunomide promoted endothelial cell viability and BBB model integrity in an *in vitro* model

Based on the above finding, we proposed that teriflunomide had direct effects on endothelial cells. To confirm this hypothesis, human brain microvascular endothelial cells (HBMECs) were cultured and treated with different concentrations of teriflunomide. The results of Cell Counting Kit 8 (CCK8) experiments showed that 20 μM and 30 μM teriflunomide treatment significantly improved the cell viability of HBMECs (Fig. 3A). Interestingly, we compared the effects on HBMCs of three DMT drugs fingolimod, dimethyl fumarate and teriflunomide in a certain concentration range and found that only teriflunomide had a positive effect on viability (Additional file 1: Fig. S1). Then we established an *in vitro* BBB model with HBMECs. The TEER and the transmittance of sodium fluorescein (NaF) were measured to evaluate BBB integrity [23]. As shown in Fig. 3B and C, 20 μM and 30 μM teriflunomide significantly increased the TEER and reduced the transmittance of NaF, suggesting that teriflunomide promoted BBB integrity in this model system.

To examine the protective effect of teriflunomide on HBMECs, we used tumor necrosis factor (TNF) and interferon-γ (IFN-γ) to induce inflammatory injury[24]. After inflammatory cytokine treatment, the viability of HBMCs was decreased, while 30 μM teriflunomide rescued the inflammatory damage to the HBMCs (Fig. 3D). The BBB model showed that TEER was reduced (Fig. 3E), and the transmittance of NaF (Fig. 3F) was increased after inflammatory cytokine injury. However, the trends were reversed by 30 μM

teriflunomide. This part of the study indicated that the integrity of the BBB model was damaged when inflammation occurred, while teriflunomide could improve HBMECs recovery after inflammatory injury.

Mannitol (also called as E421) has been reported to temporarily open the BBB[25]. We tested the cell-damaging effects of E421, a noninflammatory stimulus, on HBMECs. The concentrations of 100 and 300 mM E421 caused decreased cell viability (Additional file 2: Fig. S2). Both 20 and 30 μM teriflunomide improved the condition of HBMECs (Fig. 3G). We further measured the TEER of the BBB model and the transmittance of NaF. E421 (100 mM) resulted in a reduction in TEER (Fig. 3H), which led to an increase in the transmittance of NaF (Fig. 3I). ABoth TEER and transmittance recovered after 30 μM teriflunomide treatment.

The results of HBMECs and BBB model *in vitro* showed that teriflunomide had direct effects on endothelial cells.

Teriflunomide upregulates the expression of claudin-1 in HBMECs

Since we observed that teriflunomide increased the TJ protein claudin-5 level in EAE rats, we next examined the effects of teriflunomide treatment on the expression of various genes encoding TJ proteins. As shown in Fig. 4A, teriflunomide significantly upregulated the expression of claudin-1 and promoted other claudin family member levels which expressed in the BBB (claudin-5 and claudin-12)[26]. However, there were no differences among other TJ proteins, such as ZO-1 and occludin (Additional file 3: Fig. S3A, B). Claudins are cell-cell adhesion molecules located at the TJs between cells in epithelial cell sheets and are responsible for the paracellular barrier function of TJs[27]. Among them, claudin-1 has been reported to increase in response to injury, resulting in augmented leakiness of the BBB[28]. Therefore, the regulation of claudin-1 by teriflunomide may be responsible for the protective effect on the BBB.

Western blot results demonstrated that the protein level of claudin-1 was upregulated by teriflunomide (Fig. 4B, C). Immunofluorescence images showed that 30 μM teriflunomide increased claudin-1 expression in HBMECs (Fig. 4D, E). Since there was little difference in the treatment results of the 20 and 30 μM teriflunomide, the following studies were carried out with 30 μM teriflunomide. These data demonstrated that teriflunomide significantly increased the expression of claudin-1.

Then we investigated whether claudin-1 was necessary for the regulation of BBB by teriflunomide. After transfection with an siRNA targeting *CDLN1* (si*CLDN1*) transfection, claudin-1 expression was greatly reduced in HBMECs (Additional file 4: Fig. S4A, B). Reduction of claudin-1 prevented the increase in BBB model TEER in the teriflunomide-treated group (Fig. 4F), and the transmittance of NaF was also similar to that observed in the control group (Fig. 4G). These findings suggested the promotion of BBB integrity by teriflunomide was due to claudin-1.

Teriflunomide upregulated the Wnt signaling pathway in HBMECs

To investigate the regulatory effect of teriflunomide on endothelial cell genes and signaling pathways, RNA sequencing was performed (Fig. 5A). The results of RNA sequencing also revealed that *CLDN1* was

significantly upregulated after the teriflunomide treatment (Additional file 5: Fig. S5A). In addition to the energy and metabolic changes associated with the DHODH enzyme function, we also screened for signal transduction pathways affected by teriflunomide (Fig. 5B). Among these, we selected the Wnt signaling pathway for further study because Wnt has been reported to be related to TJ expression and BBB integrity (Additional file 5: Fig. S5B)[29, 30]. Wnt2b, a member of the Wnt family, functions in a variety of developmental processes, including cell growth[31]. CKI-ε is a Wnt-regulated kinase and participates in the phosphorylation of Dvl, allowing for control of the Wnt/β-catenin signaling pathway[32]. The promotion of Wnt signaling by teriflunomide might be responsible for the upregulation of claudin-1. We confirmed the upregulation of Wnt2b by teriflunomide treatment at the RNA (Fig. 5C, D) and protein levels (Fig. 5E). In addition, the spinal cords of teriflunomide-treated EAE rats also showed a significant increase in Wnt2b. These results suggested teriflunomide mediated on Wnt signaling.

The promotion of BBB integrity by teriflunomide is due to Wnt signaling

To prove that teriflunomide finctions through the Wnt/β-catenin pathway, two inhibitors, LGK974 and IWR-1, were added to cultured HBMECs. LGK974 inhibited Wnt secretion, and IWR-1 prevented β-catenin dissociation by inducing axin protein stabilization, corresponding to events upstream and downstream of Wnt/β-catenin signaling[33, 34]. After inhibitor addition, the increase in *CLDN1* gene expression induced by teriflunomide was significantly suppressed (Fig. 6A). Western blot results indicated that the decreased in claudin-1 expression was related to β-catenin following inhibitor treatment (Fig. 6B-D). Immunofluorescence also showed a reduction in claudin-1 in HBMECs (Fig. 6E, F). In addition, Wnt inhibitors decreased the TEER (Fig. 6G) and increased the transmittance of NaF (Fig. 6H), demonstrating that the regulation of BBB integrity by teriflunomide was disrupted by treatment with inhibitors.

Meanwhile, HBMECs were transfected with siRNAs targeting *CTNB* (the gene for β-catenin) to further confirm that teriflunomide functions through Wnt/β-catenin signaling. First, it was confirmed that si*CTNB* reduced β-catenin expression (Fig. 6I). si*CTNB* also suppressed the upregulation of cluadin-1 by teriflunomide (Fig. 6I-L). β-catenin knockdown in the BBB model made it unresponsive to teriflunomide treatment (Fig. 6M, N). These data further illustrated the importance of Wnt/β-catenin signaling on the effect of teriflunomide function in HBMECs.

Activation of Wnt signaling promoted BBB integrity *in vitro* and *in vivo*.

Since we showed that teriflunomide maintained the permeability of that BBB through the Wnt/β-catenin pathways, we wondered whether activation of Wnt/β-catenin signaling would have the same function as teriflunomide. Two Wnt signaling agonists r-spondin1 and SKL2001 were chosen for this part of the study. R-spondin1 bound to the Wnt coreceptors and SKL2001 disrupted the β-catenin/Axin interaction for upstream and downstream activation of the Wnt/β-catenin pathway[35, 36].

Similar to teriflunomide, the gene (Fig. 7A) and protein (Fig. 7B, C) levels of claudin-1 were significantly increased after treatment with each agonist, corresponding with β-catenin expression (Fig. 7B, D). In addition, agonists also promoted claudin-1 expression in HBMECs (Fig. 7E, F), suggesting that activation

of Wnt signaling could affect tight junctions. Therefore, we examined the effect of agonists on the BBB model *in vitro* and found that both could improve TEER (Fig. 7G) and reduce NaF penetration (Fig. 7H). These data indicated that the activation of Wnt signaling promoted the integrity of the BBB.

We further investigated the protective effect of agonists on the BBB damaged by inflammation First, the BBB model was treated with inflammatory cytokines, then Wnt agonists were added. TEER recovered under Wnt signaling activation (Fig. 7I), and the transmittances of NaF was also decreased (Fig. 7J).

Since r-spondin1 had a more significant promoting effect on HBMECs, we treated EAE rats with r-spondin1 by intravenous tail injections. We observed that r-spondin1decreased the clinical scores of EAE rats (Fig. 7K). Moreover, r-spondin1 reduced the penetration of Evans blue into the CNS (Fig. 7L, M). Peripheral leakage of NFLs from the CNS was also improved (Fig. 7N). The decreases in BBB injuries in the r-spondin1 group was consistent with the alleviation of spinal cord demyelination (Fig. 7O). These results indicated that the Wnt agonist could reduce BBB damage and ameliorate EAE progression.

In addition, the activation of Wnt/β-catenin signaling was detected by immunofluorescence. As with the TJ proteins measured in the previous experiment, claudin-1 expression in spinal cord was decreased after EAE induction (Fig. 7P, Q), suggesting serious BBB damage. Teriflunomide significantly promoted the expression of Wnt2b and β-catenin, which correlated with an increase in claudin-1 (Fig. 7P-S). R-spondin1 directly activated β-catenin and led to the recovery of claudin-1 expression (Fig. 7P-S). These data demonstrated that activation of the Wnt/β-catenin pathway could maintain BBB integrity through upregulation of claudin-1 expression.

Discussion

In this study, we demonstrate that teriflunomide has an effect on BBB protection by promoting claudin-1 expression, which is associated with the activation of Wnt signaling.

The structure of the BBB preserves the CNS homeostatic process and prevents the entry of potentially neurotoxic substances into the brain, including peripheral immune cells and pathogens[37]. Based on human tissue and animal models, the massive infiltration of immune cells into the CNS usually accompanies the disruption of the BBB[38, 39]. However, the BBB has very complex components, particularly endothelial cells and TJs. The injured BBB with defective TJs fails to stop autoreactive leukocyte trafficking into brain lesions by a mechanism that has become increasingly understood[40]. Previous studies revealed that gadolinium enhancing lesions revealed by MRI were positively correlated with active lesions and the clinical relapse of MS. MRI gadolinium enhancing lesions imply increased permeability and abnormal TJs of the BBB with autoimmune cell-induced demyelinating plaques[41]. Studies have revealed that the permeability of the BBB measured by MRI is significantly correlated with NFLs in serum, providing novel pathological and inflammatory information for MS[17]. The development of drugs to restore the defective BBB has been the focus of research for many decades. It has been demonstrated that the important function of glucocorticoid treatment during the acute stage of MS is to repair the damaged BBB, preventing escalation of inflammatory

demyelinating[42]. All these drugs protect the BBB indirectly by inhibiting the infiltration of inflammatory cells, and few have reported direct effects on BBB integrity.

Current knowledge about teriflunomide is limited to inhibiting DHODH, active T-cell proliferation, and cytokine release. However, its functions are not limited to this; for example, teriflunomide has been reported to significantly promote myelin regeneration[43] . Based on our clinical studies, we found that teriflunomide repaired the defective BBB in MS. Teriflunomide significantly reduced serum NFL leakage, which is a valuable marker for BBB integrity in MS. A correlation between BBB permeability and perivascular inflammatory cuffing was observed at an early stage in an EAE marmoset model[44]. These findings are consistent with our current study: Markedly increased extravasation of Evans blue and subsequent NFL release were detected following the induction of EAE, confirming that BBB integrity was compromised. These studies demonstrated that teriflunomide had a protective effect by reducing BBB leakage in clinical and animal studies. Whether this observation is based on direct effects on the BBB is not conclusive. Therefore, endothelial cells, an important component of the BBB, were selected to study the effects of teriflunomide *in vitro*. We observed markedly increased TEER and decreased transmittance of NaF in HBMECs after teriflunomide treatment. Teriflunomide had the same protective effects on inflammation and mannitol injury models. These results revealed that teriflunomide had a protective role in the reestablishment of the damaged BBB.

Protecting the homeostasis and physiological function of brain tissue is based on a multitude of interactions between its components, including TJs, endothelial cells, astrocytes and pericytes. However, the BBB is mainly sealed by endothelial cells and their paracellular TJs. TJs are the major component of the junction complex, forming a seal in endothelial cells to prevent solutes from undergoing paracellular diffusion and to mediate the gate function of the BBB. Loss of TJs leads to BBB breach and increases the permeability of the BBB[9, 45]. Claudin proteins are an important group of TJs critical to intercellular tight junction formation and BBB integrity. A study reported that the endothelial cells of the BBB mostly express claudin-1, claudin-3, claudin-5 and claudin-12[26]. We found that teriflunomide increased the expression of claudin1 in HBMECs, suggesting that teriflunomide could protect the BBB by upregulating claudin1 expression.

Claudin-1 is an integral protein in TJ formation. Genetic disruption of *CLDN* results in breakdown of the epithelial barrier and neonatal death (within 1 day of birth), accompanied by excessive transepidermal water loss[46]. However, loss of claudin-1 only alters the BBB junctional properties to induce tracer leakage in a size-selective manner but does not result in a complete breakdown[47]. Given that TJs are the characteristic features shared by the BBB and epithelial barrier, these data suggest that claudin-1 is essential for the integrity of the BBB. We also conducted *siCLDN1* experiments in this study to further illustrate this point.

The Wnt/β-catenin pathway is activated in endothelial cells during embryogenesis but not in nonneural tissues, and therefore it drives angiogenesis specifically in the CNS[48]. The Wnt pathway also has a central role in BBB formation and repair[49]. Therefore, the same signal that drives endothelial cell

migration into the CNS also has BBB functions, suggesting a CNS-specific angiogenic program that imparts barrier-specific properties to the vasculature. Endothelia β-catenin also has a key role in embryonic and postnatal BBB maturation by regulating the formation of TJs, and the increased expression of claudin-1 has been proposed to be involved in this process[50]. We found that teriflunomide promoted the Wnt signaling pathway by RNA-sequencing and verified it in HBMECs. Our results demonstrate the regulation of claudin-1 driven by teriflunomide effects on Wnt signaling.

Conclusion

Our study revealed that teriflunomide upregulated the expression of the tight junction protein claudin-1 in endothelial cells, and promoted the integrity of BBB through Wnt signaling (Fig.8). This work reveals a novel mechanism of teriflunomide in neuroinflammatory diseases with BBB injuries.

Abbreviations

BBB: Blood-brain barrier; CCK8: Cell Counting Kit 8; CNS: Central nervous system; DCE-MRI: Dynamic contrast enhanced magnetic resonance imaging; DHODH: Dihydroorotate dehydrogenase; DMTs: Disease-modifying therapies; EAE: Experiment autoimmune encephalomyelitis; HBMECs: Human brain microvascular endothelial cells; HRP: Horseradish peroxidase; IFN-γ: Interferon-γ; LFB: Luxol fast blue; MS: Multiple sclerosis; NaF: Sodium fluorescein; NFLs: Neurofilament light chains; PBS: Phosphate-buffered saline; RRMS: Relapsing-remitting multiple sclerosis; SOCE: Store-operated calcium entry; TEER: Transendothelial electrical resistance; TER: Teriflunomide; TNF: Tumor necrosis factor; TJs: Tight junctions; ZO: Zonula occludens.

Declarations

Supplementary Information

Additional file **Fig.S1.** Cytotoxicity of fingolimod, dimethyl fumarate or teriflunomide on HBMECs. **Fig.S2.** Cytotoxicity of mannitol on HBMECs. **Fig.S3.** The effects of teriflunomide on HBMECs TJ proteins expression. **Fig.S4.** The siclaudin-1 RNA effect on HBMECs claudin-1 expression. **Fig.S5.** The effect of teriflunomide on TJ proteins expressions and Wnt signaling by RNA sequencing analysis.

Acknowledgements

Not applicable.

Author contributions

QW conceived the project. ZY designed the experiments and wrote the manuscript. FL, CY and WJ contributed to the clinical samples collection and analysis. CC, XX, CX, PF, SS and WS conducted the experiments. CW edited the manuscript.

Funding

This work was financially supported by the National Natural Science Foundation of

China (32070962, 81771300, 81971140, 82001284, 82101418), the Chinese Postdoctoral Science Foundation (2020M672994), Natural Science Foundation of Guangdong Province (2020A1515010053)

Availability of data and materials

The datasets during and/or analyzed during the current study are available from the corresponding author on reasonable request.

Ethics approval and consent to participate

This study was authorized by the Sun Yat-sen University Ethics Committee. Written informed consent was obtained from all the MS patients and animal experiments were performed in conformity to the guidelines of the National Institutes of Health on the care and use of animals.

Consent for publication

Not applicable.

Competing interests

The authors declare that they have no competing interests.

Author details

[1]Department of Neurology, The Third Affiliated Hospital of Sun Yat-sen University, Guangzhou, 510000, China. [2]The Center of Mental and Neurological Disorders Study, The Third Affiliated Hospital of Sun Yat-sen University, Guangzhou, 510000, China. [3]Shenzhen Key Laboratory of Cardiovascular Disease, Fuwai Hospital Chinese Academy of Medical Sciences, Shenzhen, 518057, China. [4]Department of Radiology, The Third Affiliated Hospital of Sun Yat-sen University, Guangzhou, 510000, China.

References

1. Filippi M, Bar-Or A, Piehl F, Preziosa P, Solari A, Vukusic S, Rocca MA. Multiple sclerosis. Nat Rev Dis Primers. 2018; 4:43.
2. Niu J, Tsai HH, Hoi KK, Huang N, Yu G, Kim K, Baranzini SE, Xiao L, Chan JR, Fancy SPJ. Aberrant oligodendroglial-vascular interactions disrupt the blood-brain barrier, triggering CNS inflammation. Nat Neurosci. 2019; 22:709-718.
3. Tintore M, Vidal-Jordana A, Sastre-Garriga J. Treatment of multiple sclerosis - success from bench to bedside. Nat Rev Neurol. 2019; 15:53-58.

4. Amato MP, Fonderico M, Portaccio E, Pasto L, Razzolini L, Prestipino E, Bellinvia A, Tudisco L, Fratangelo R, Comi G, et al. Disease-modifying drugs can reduce disability progression in relapsing multiple sclerosis. Brain. 2020; 143:3013-3024.
5. Rollot F, Casey R, Leray E, Debouverie M, Edan G, Wiertlewski S, Vukusic S, Laplaud DA. Cumulative effects of therapies on disability in relapsing multiple sclerosis. Mult Scler. 2021; 27:1760-1770.
6. Gunduz T, Kurtuncu M, Eraksoy M. Severe rebound after withdrawal of fingolimod treatment in patients with multiple sclerosis. Mult Scler Relat Disord. 2017; 11:1-3.
7. Munji RN, Soung AL, Weiner GA, Sohet F, Semple BD, Trivedi A, Gimlin K, Kotoda M, Korai M, Aydin S, et al. Profiling the mouse brain endothelial transcriptome in health and disease models reveals a core blood-brain barrier dysfunction module. Nat Neurosci. 2019; 22:1892-1902.
8. Mandel I, Paperna T, Glass-Marmor L, Volkowich A, Badarny S, Schwartz I, Vardi P, Koren I, Miller A. Tight junction proteins expression and modulation in immune cells and multiple sclerosis. J Cell Mol Med. 2012; 16:765-775.
9. Cayrol R, Wosik K, Berard JL, Dodelet-Devillers A, Ifergan I, Kebir H, Haqqani AS, Kreymborg K, Krug S, Moumdjian R, et al. Activated leukocyte cell adhesion molecule promotes leukocyte trafficking into the central nervous system. Nat Immunol. 2008; 9:137-145.
10. Graesser D, Solowiej A, Bruckner M, Osterweil E, Juedes A, Davis S, Ruddle NH, Engelhardt B, Madri JA. Altered vascular permeability and early onset of experimental autoimmune encephalomyelitis in PECAM-1-deficient mice. J Clin Invest. 2002; 109:383-392.
11. Confavreux C, O'Connor P, Comi G, Freedman MS, Miller AE, Olsson TP, Wolinsky JS, Bagulho T, Delhay JL, Dukovic D, et al. Oral teriflunomide for patients with relapsing multiple sclerosis (TOWER): a randomised, double-blind, placebo-controlled, phase 3 trial. Lancet Neurol. 2014; 13:247-256.
12. Miller AE, Wolinsky JS, Kappos L, Comi G, Freedman MS, Olsson TP, Bauer D, Benamor M, Truffinet P, O'Connor PW, Group TS. Oral teriflunomide for patients with a first clinical episode suggestive of multiple sclerosis (TOPIC): a randomised, double-blind, placebo-controlled, phase 3 trial. Lancet Neurol. 2014; 13:977-986.
13. Rahman S, Rahman T. Unveiling some FDA-approved drugs as inhibitors of the store-operated Ca(2+) entry pathway. Sci Rep. 2017; 7:12881.
14. Jiang L, Zhang W, Li W, Ling C, Jiang M. Anti-inflammatory drug, leflunomide and its metabolite teriflunomide inhibit NSCLC proliferation in vivo and in vitro. Toxicol Lett. 2018; 282:154-165.
15. Hail N, Jr., Chen P, Kepa JJ, Bushman LR. Evidence supporting a role for dihydroorotate dehydrogenase, bioenergetics, and p53 in selective teriflunomide-induced apoptosis in transformed versus normal human keratinocytes. Apoptosis. 2012; 17:258-268.
16. Bittner S, Ruck T, Schuhmann MK, Herrmann AM, Moha ou Maati H, Bobak N, Gobel K, Langhauser F, Stegner D, Ehling P, et al. Endothelial TWIK-related potassium channel-1 (TREK1) regulates immune-cell trafficking into the CNS. Nat Med. 2013; 19:1161-1165.
17. Bittner S, Oh J, Havrdova EK, Tintore M, Zipp F. The potential of serum neurofilament as biomarker for multiple sclerosis. Brain. 2021; 144:2954-2963.

18. Uher T, McComb M, Galkin S, Srpova B, Oechtering J, Barro C, Tyblova M, Bergsland N, Krasensky J, Dwyer M, et al. Neurofilament levels are associated with blood-brain barrier integrity, lymphocyte extravasation, and risk factors following the first demyelinating event in multiple sclerosis. Mult Scler. 2021; 27:220-231.
19. Umeda K, Ikenouchi J, Katahira-Tayama S, Furuse K, Sasaki H, Nakayama M, Matsui T, Tsukita S, Furuse M, Tsukita S. ZO-1 and ZO-2 independently determine where claudins are polymerized in tight-junction strand formation. Cell. 2006; 126:741-754.
20. Greene C, Kealy J, Humphries MM, Gong Y, Hou J, Hudson N, Cassidy LM, Martiniano R, Shashi V, Hooper SR, et al. Dose-dependent expression of claudin-5 is a modifying factor in schizophrenia. Mol Psychiatry. 2018; 23:2156-2166.
21. Furuse M, Hirase T, Itoh M, Nagafuchi A, Yonemura S, Tsukita S, Tsukita S. Occludin: a novel integral membrane protein localizing at tight junctions. J Cell Biol. 1993; 123:1777-1788.
22. Cramer SP, Simonsen HJ, Varatharaj A, Galea I, Frederiksen JL, Larsson HBW. Permeability of the blood-brain barrier predicts no evidence of disease activity at 2 years after natalizumab or fingolimod treatment in relapsing-remitting multiple sclerosis. Ann Neurol. 2018; 83:902-914.
23. Eigenmann DE, Xue G, Kim KS, Moses AV, Hamburger M, Oufir M. Comparative study of four immortalized human brain capillary endothelial cell lines, hCMEC/D3, hBMEC, TY10, and BB19, and optimization of culture conditions, for an in vitro blood-brain barrier model for drug permeability studies. Fluids Barriers CNS. 2013; 10:33.
24. Chui R, Dorovini-Zis K. Regulation of CCL2 and CCL3 expression in human brain endothelial cells by cytokines and lipopolysaccharide. J Neuroinflammation. 2010; 7:1.
25. Kaya M, Gulturk S, Elmas I, Kalayci R, Arican N, Kocyildiz ZC, Kucuk M, Yorulmaz H, Sivas A. The effects of magnesium sulfate on blood-brain barrier disruption caused by intracarotid injection of hyperosmolar mannitol in rats. Life Sci. 2004; 76:201-212.
26. Sweeney MD, Zhao Z, Montagne A, Nelson AR, Zlokovic BV. Blood-Brain Barrier: From Physiology to Disease and Back. Physiol Rev. 2019; 99:21-78.
27. Tsukita S, Tanaka H, Tamura A. The Claudins: From Tight Junctions to Biological Systems. Trends Biochem Sci. 2019; 44:141-152.
28. Sladojevic N, Stamatovic SM, Johnson AM, Choi J, Hu A, Dithmer S, Blasig IE, Keep RF, Andjelkovic AV. Claudin-1-Dependent Destabilization of the Blood-Brain Barrier in Chronic Stroke. J Neurosci. 2019; 39:743-757.
29. Lengfeld JE, Lutz SE, Smith JR, Diaconu C, Scott C, Kofman SB, Choi C, Walsh CM, Raine CS, Agalliu I, Agalliu D. Endothelial Wnt/beta-catenin signaling reduces immune cell infiltration in multiple sclerosis. Proc Natl Acad Sci U S A. 2017; 114:E1168-E1177.
30. Moreau N, Mauborgne A, Couraud PO, Romero IA, Weksler BB, Villanueva L, Pohl M, Boucher Y. Could an endoneurial endothelial crosstalk between Wnt/beta-catenin and Sonic Hedgehog pathways underlie the early disruption of the infra-orbital blood-nerve barrier following chronic constriction injury? Mol Pain. 2017; 13:1744806917727625.

31. Kubo F, Takeichi M, Nakagawa S. Wnt2b inhibits differentiation of retinal progenitor cells in the absence of Notch activity by downregulating the expression of proneural genes. Development. 2005; 132:2759-2770.
32. Sakanaka C. Phosphorylation and regulation of beta-catenin by casein kinase I epsilon. J Biochem. 2002; 132:697-703.
33. Jiang X, Hao HX, Growney JD, Woolfenden S, Bottiglio C, Ng N, Lu B, Hsieh MH, Bagdasarian L, Meyer R, et al. Inactivating mutations of RNF43 confer Wnt dependency in pancreatic ductal adenocarcinoma. Proc Natl Acad Sci U S A. 2013; 110:12649-12654.
34. Wei TT, Chandy M, Nishiga M, Zhang A, Kumar KK, Thomas D, Manhas A, Rhee S, Justesen JM, Chen IY, et al. Cannabinoid receptor 1 antagonist genistein attenuates marijuana-induced vascular inflammation. Cell. 2022; 185:1676-1693 e1623.
35. Jie Z, Shen S, Zhao X, Xu W, Zhang X, Huang B, Tang P, Qin A, Fan S, Xie Z. Activating beta-catenin/Pax6 axis negatively regulates osteoclastogenesis by selectively inhibiting phosphorylation of p38/MAPK. FASEB J. 2019; 33:4236-4247.
36. Liang F, Zhang H, Cheng D, Gao H, Wang J, Yue J, Zhang N, Wang J, Wang Z, Zhao B. Ablation of LGR4 signaling enhances radiation sensitivity of prostate cancer cells. Life Sci. 2021; 265:118737.
37. Langen UH, Ayloo S, Gu C. Development and Cell Biology of the Blood-Brain Barrier. Annu Rev Cell Dev Biol. 2019; 35:591-613.
38. Hawley RJ, Nemeroff CB, Bissette G, Guidotti A, Rawlings R, Linnoila M. Neurochemical correlates of sympathetic activation during severe alcohol withdrawal. Alcohol Clin Exp Res. 1994; 18:1312-1316.
39. Larochelle C, Uphaus T, Broux B, Gowing E, Paterka M, Michel L, Dudvarski Stankovic N, Bicker F, Lemaitre F, Prat A, et al. EGFL7 reduces CNS inflammation in mouse. Nat Commun. 2018; 9:819.
40. Kirk J, Plumb J, Mirakhur M, McQuaid S. Tight junctional abnormality in multiple sclerosis white matter affects all calibres of vessel and is associated with blood-brain barrier leakage and active demyelination. J Pathol. 2003; 201:319-327.
41. Saade C, Bou-Fakhredin R, Yousem DM, Asmar K, Naffaa L, El-Merhi F. Gadolinium and Multiple Sclerosis: Vessels, Barriers of the Brain, and Glymphatics. AJNR Am J Neuroradiol. 2018; 39:2168-2176.
42. Gaillard PJ, van Der Meide PH, de Boer AG, Breimer DD. Glucocorticoid and type 1 interferon interactions at the blood-brain barrier: relevance for drug therapies for multiple sclerosis. Neuroreport. 2001; 12:2189-2193.
43. Gottle P, Manousi A, Kremer D, Reiche L, Hartung HP, Kury P. Teriflunomide promotes oligodendroglial differentiation and myelination. J Neuroinflammation. 2018; 15:76.
44. Maggi P, Macri SM, Gaitan MI, Leibovitch E, Wholer JE, Knight HL, Ellis M, Wu T, Silva AC, Massacesi L, et al. The formation of inflammatory demyelinated lesions in cerebral white matter. Ann Neurol. 2014; 76:594-608.
45. Camara-Lemarroy CR, Silva C, Greenfield J, Liu WQ, Metz LM, Yong VW. Biomarkers of intestinal barrier function in multiple sclerosis are associated with disease activity. Mult Scler. 2020; 26:1340-

1350.

46. Furuse M, Hata M, Furuse K, Yoshida Y, Haratake A, Sugitani Y, Noda T, Kubo A, Tsukita S. Claudin-based tight junctions are crucial for the mammalian epidermal barrier: a lesson from claudin-1-deficient mice. J Cell Biol. 2002; 156:1099-1111.
47. Pfeiffer F, Schafer J, Lyck R, Makrides V, Brunner S, Schaeren-Wiemers N, Deutsch U, Engelhardt B. Claudin-1 induced sealing of blood-brain barrier tight junctions ameliorates chronic experimental autoimmune encephalomyelitis. Acta Neuropathol. 2011; 122:601-614.
48. Guo R, Wang X, Fang Y, Chen X, Chen K, Huang W, Chen J, Hu J, Liang F, Du J, et al. rhFGF20 promotes angiogenesis and vascular repair following traumatic brain injury by regulating Wnt/beta-catenin pathway. Biomed Pharmacother. 2021; 143:112200.
49. Martin M, Vermeiren S, Bostaille N, Eubelen M, Spitzer D, Vermeersch M, Profaci CP, Pozuelo E, Toussay X, Raman-Nair J, et al. Engineered Wnt ligands enable blood-brain barrier repair in neurological disorders. Science. 2022; 375:eabm4459.
50. Lippmann ES, Azarin SM, Kay JE, Nessler RA, Wilson HK, Al-Ahmad A, Palecek SP, Shusta EV. Derivation of blood-brain barrier endothelial cells from human pluripotent stem cells. Nat Biotechnol. 2012; 30:783-791.

Table 1

Table.1 Characteristics of MS patients participated in the DCE-MRI study. The information about ages, sex and disease development processes were listed.

Group	Patients Number	Treatment	Age (years)	Sex	Disease Duration	EDSS	Relapse times	K^{trans} (min^{-1})
Control MS	1	None	33	F	6	2.5	3	0.1265
	2	None	36	F	9	2.5	4	0.098
	3	Fingolimod for 6 month	25	F	6	3	5	0.13
TER (1-3)	4	Teriflunomide for 1 month	43	F	9	3.5	3	0.129
	5	Teriflunomide for 3 month	31	M	3	3	2	0.0135
	6	Teriflunomide for 3 month	42	M	12	2	2	0.483
TER (over 6)	6	Teriflunomide for 6 month	42	M	12	2	2	0.024
	7	Teriflunomide for 7 month	34	F	2	2	3	0.013
	8	Teriflunomide for 2 year	23	F	4	1	5	0.013
	9	Teriflunomide for 1 year	22	F	2	2	1	0.0105
	10	Teriflunomide for 6 month	40	F	6	1.5	4	0.094
	11	Teriflunomide for 6month	29	M	8	2	6	0.014

Figures

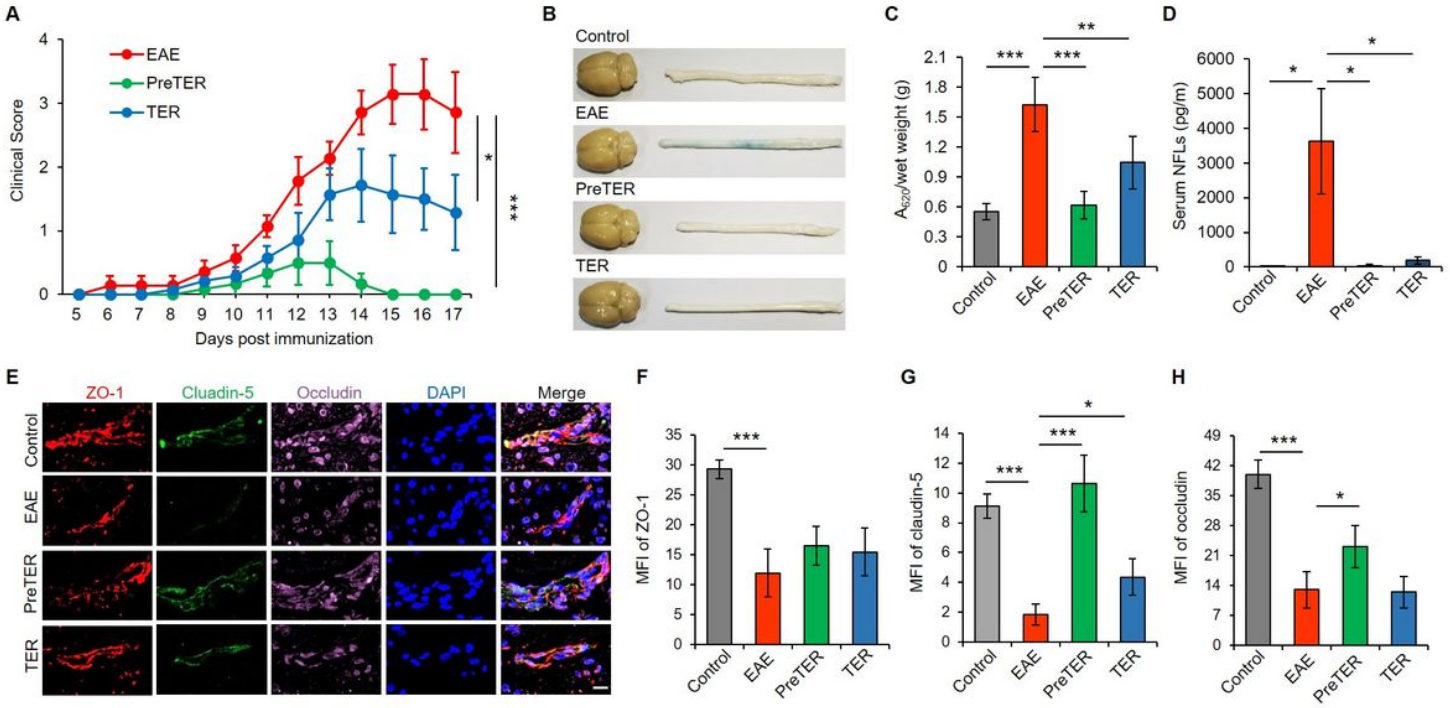

Figure 1

TER protected BBB integrity in EAE model. (**A**) Clinical scores of EAE rats without or with TER. Error bars represent ± s.e.m. (n = 7). (**B**) Extravasation of Evans blue into the CNS 24 h after intravenous injection and (**C**) quantification analysis. Error bars represent ± s.e.m. (n = 4). (**D**) Detection of NFLs in the rat serum after the experiments. Error bars represent ± s.e.m. (n = 3). (**E**)The immunofluorescence images and quantitative analysis of (**F**) ZO-1, (**G**) claudin-5 and (**H**) occludin in the spinal cords. Scale bar: 10 μm. Error bars represent ± s.e.m. (n = 4). Statistical significance of clinical scores was analyzed by the generalized equation, and others were assessed by ANOVA with Newman-Keuls test. *p 0.05, **p 0.01, ***p 0.001.

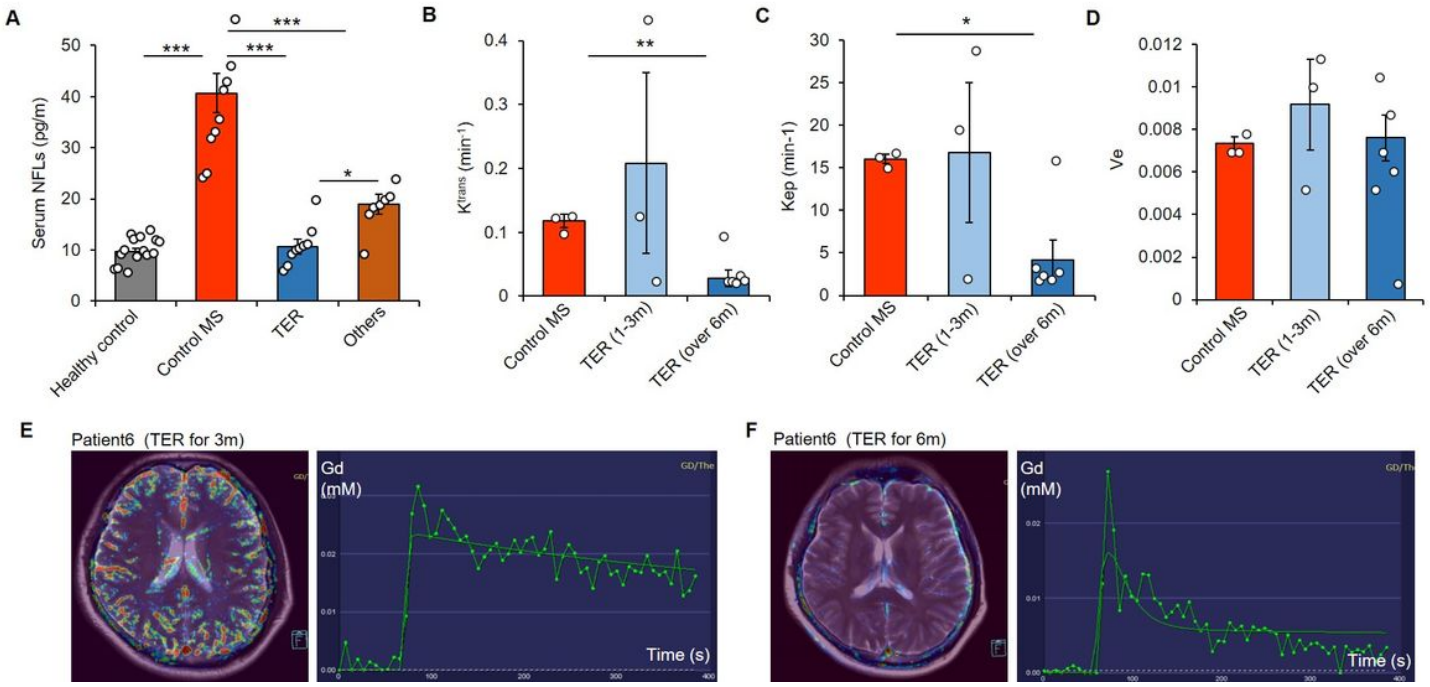

Figure 2

Teriflunomide restore the BBB in MS patients. (A) The concentrations of NFLs in the serum from each group. The (B) K^{trans}, (C) Kep and (D) Ve value of each group were measured form DCE-MRI. The comparison of DCE-MRI images (left) and K^{trans} curves (right) of MS patients treat with teriflunomide for (E) 3 months and (F) 6 months. Statistical significances were assessed by ANOVA with Newman-Keuls test. *p 0.05, **p 0.01, ***p 0.001.

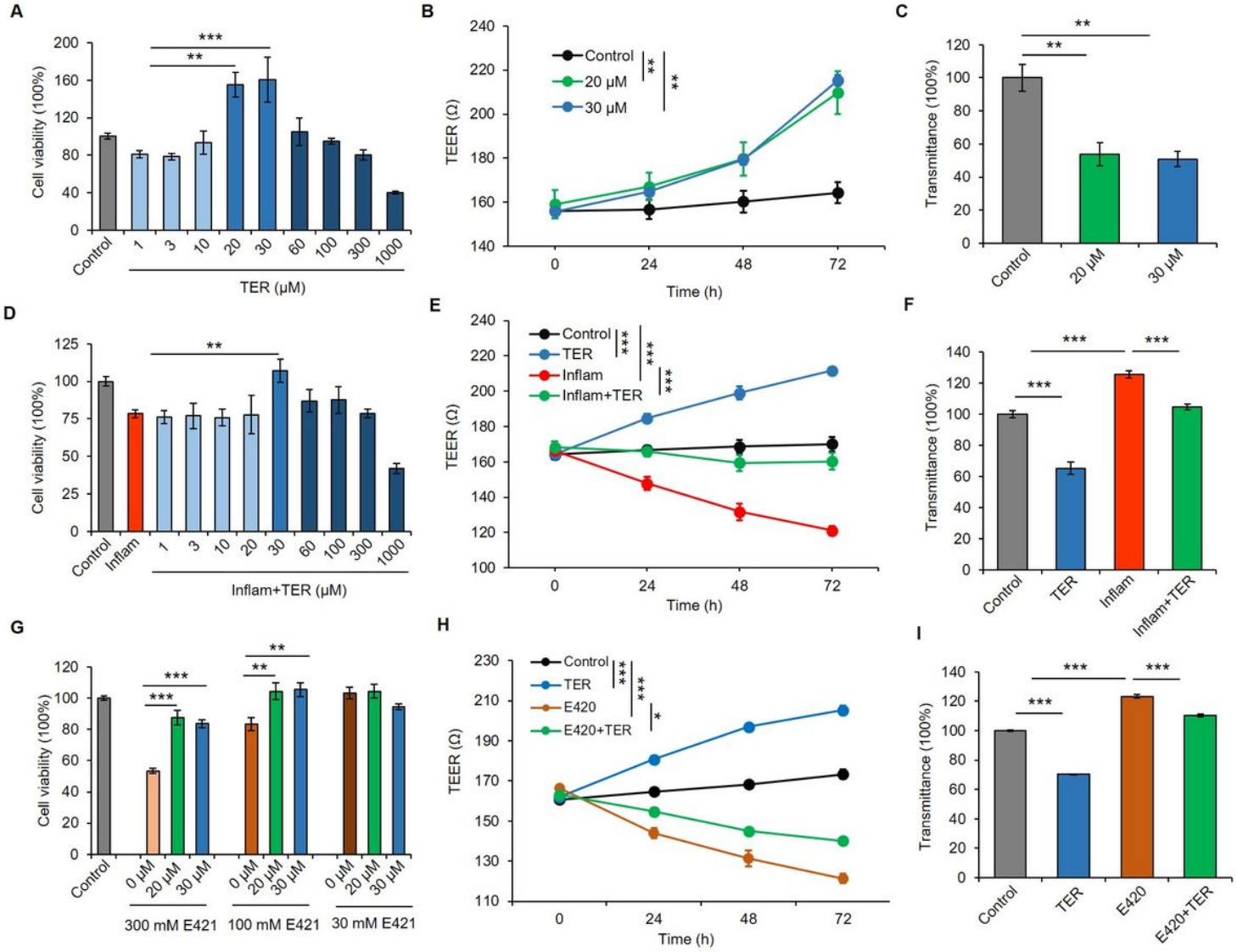

Figure 3

TER promoted BBB integrity in BBB model *in vitro*. (**A**) Cytotoxicity of different concentrations of TER to HBMECs for 48 h. Error bars represent ± s.e.m. (n = 3). (**B**) The TEER of HBMECs BBB model over 3 d with TER treatment and (**C**) transmittance of NAF after the experiment. Error bars represent ± s.e.m. (n = 3). (**D**) Cytotoxicity of pro-inflammatory cytokines without or with TER to HBMECs. LRGT Various concentrations of TER were added in the HBMECs together with cytokines for 48 h. Error bars represent ± s.e.m. (n = 3). (**E**) The TEER of inflammatory injury BBB model over 3 d without or with TER treatment and (**F**) transmittance of NAF after the experiment. Error bars represent ± s.e.m. (n = 3). (**G**) The protective effects of teriflunomide on HBMECs from different concentrations of mannitol injuries for 48 h. Error bars represent ± s.e.m. (n = 3). (H) The TEER of mannitol injury BBB model over 3 d without or with teriflunomide treatment and (**I**) transmittance of NAF after the experiment. Error bars represent ± s.e.m. (n = 3). Statistical significances were assessed by ANOVA with Newman-Keuls test. **p* 0.05, ***p* 0.01, ****p* 0.001.

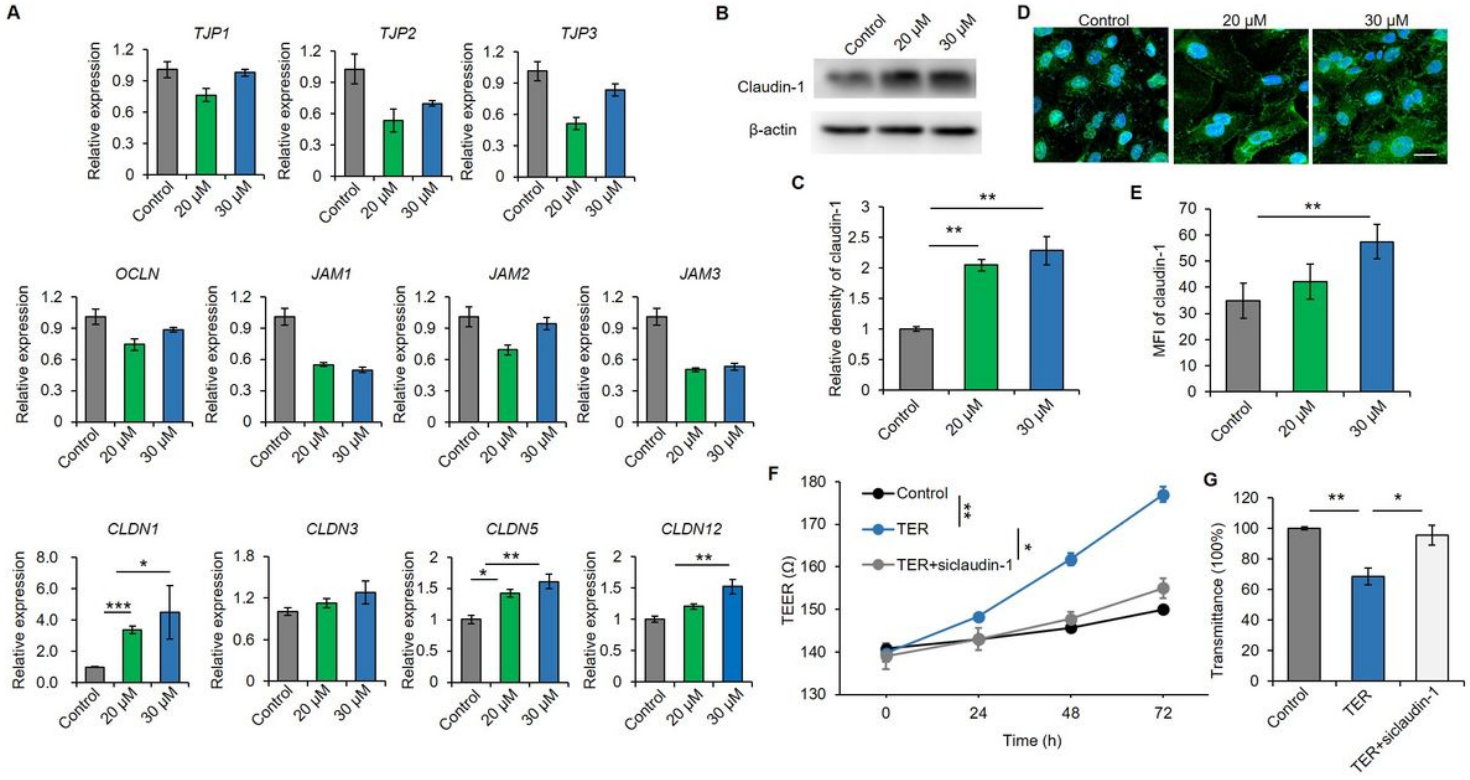

Figure 4

TER up-regulated claudin-1expression to promote BBB integrity. (**A**) Gene expressions of various TJ proteins determined by quantitative PCR. Error bars represent ± s.e.m. (n = 4). (**B**) Western blot images and (**C**) quantitative analysis of claudin-1 in HBMECs. Error bars represent ± s.e.m. (n = 3). (**D**) Confocal images and (**E**) quantitative analysis of claudin-1 in HBMECs. Scale bar: 20 μm. Error bars represent ± s.e.m. (n = 3). (F) The TEER of HBMECs BBB model over 3 d with claudin-1 knockdown and (**G**) transmittance of NAF after the experiment. Error bars represent ± s.e.m. (n = 3). Statistical significances were assessed by ANOVA with Newman-Keuls test. *p 0.05, **p 0.01.

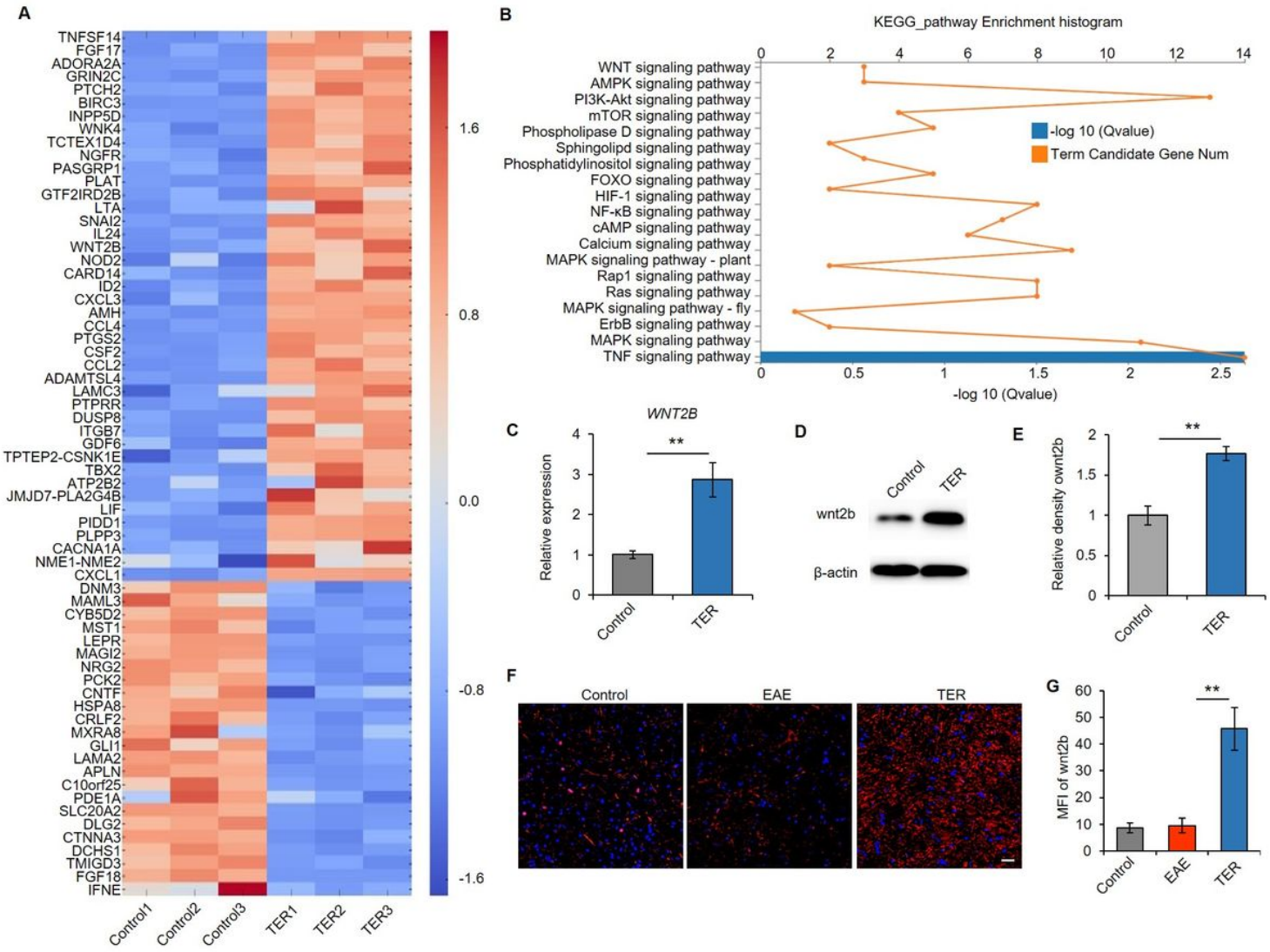

Figure 5

TER up-regulated Wnt signaling pathway by RNA-sequencing analysis. (**A**) Differentially expressed genes of control and TER group were displayed by RNA-sequencing screening. (**B**) Differentially expressed signaling pathways of control and TER group were displayed by KEGG enrichment analysis. (**C**) Gene expressions of Wnt2b determined by quantitative PCR. Error bars represent ± s.e.m. (n = 3). (**D**) Western blot images and (**E**) quantitative analysis of Wnt2b in HBMECs. Error bars represent ± s.e.m. (n = 3). (**F**) Confocal images and (**G**) quantitative analysis of Wnt2b in rat spinal cords. Scale bar: 50 μm. Error bars represent ± s.e.m. (n = 3). Statistical significances were assessed by Student t-test or ANOVA with Newman-Keuls test. ***p* 0.01.

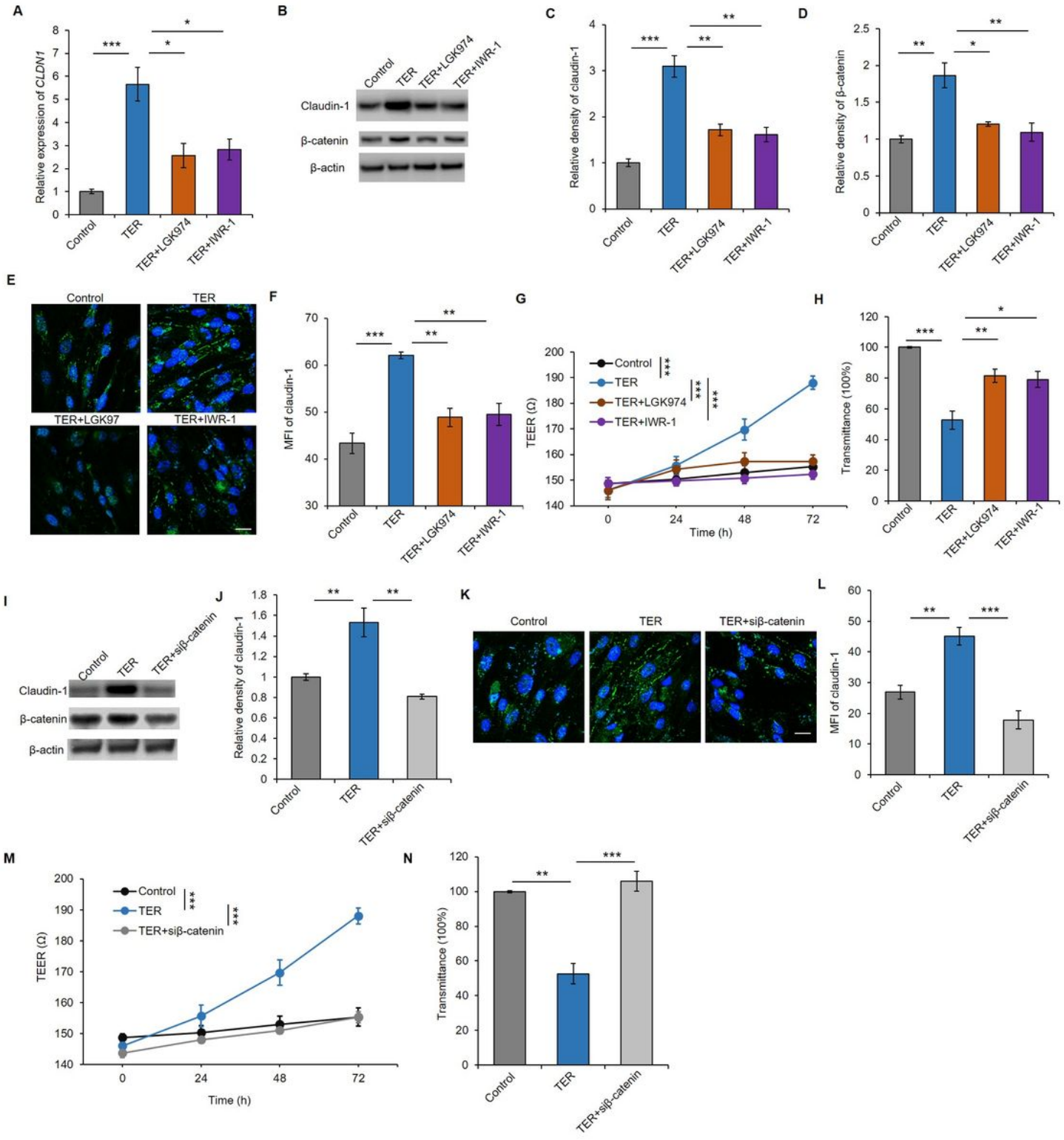

Figure 6

TER promoted claudin-1 expression through Wnt singaling. (**A**) Gene expressions of *CLDN1* determined by quantitative PCR. Error bars represent ± s.e.m. (n = 3). (**B**) Western blot images and quantitative analysis of (**C**) claudin-1 and (**D**) β-catenin in HBMECs. Error bars represent ± s.e.m. (n = 3). (**E**) Confocal images and (**F**) quantitative analysis of claudin-1 in HBMECs. Scale bar: 20 μm. Error bars represent ± s.e.m. (n = 3). (**G**) The TEER of HBMECs BBB model over 3 d with TER and Wnt inhibitors and (**H**)

transmittance of NAF after the experiment. Error bars represent ± s.e.m. (n = 3). (**I**) Western blot images and (**J**) quantitative analysis of claudin-1 in HBMECs. Error bars represent ± s.e.m. (n = 3). (**K**) Confocal images and (**L**) quantitative analysis of claudin-1 in the HBMECs with teriflunomide treatment. Scale bar: 20 μm. (**M**) The TEER of BBB model over 3 d after β-catenin knockdown and (**N**) transmittance of NAF after the experiment. Error bars represent ± s.e.m. (n = 3). Statistical significances were assessed by ANOVA with Newman-Keuls test. **p* 0.05,***p* 0.01, ****p* 0.001.

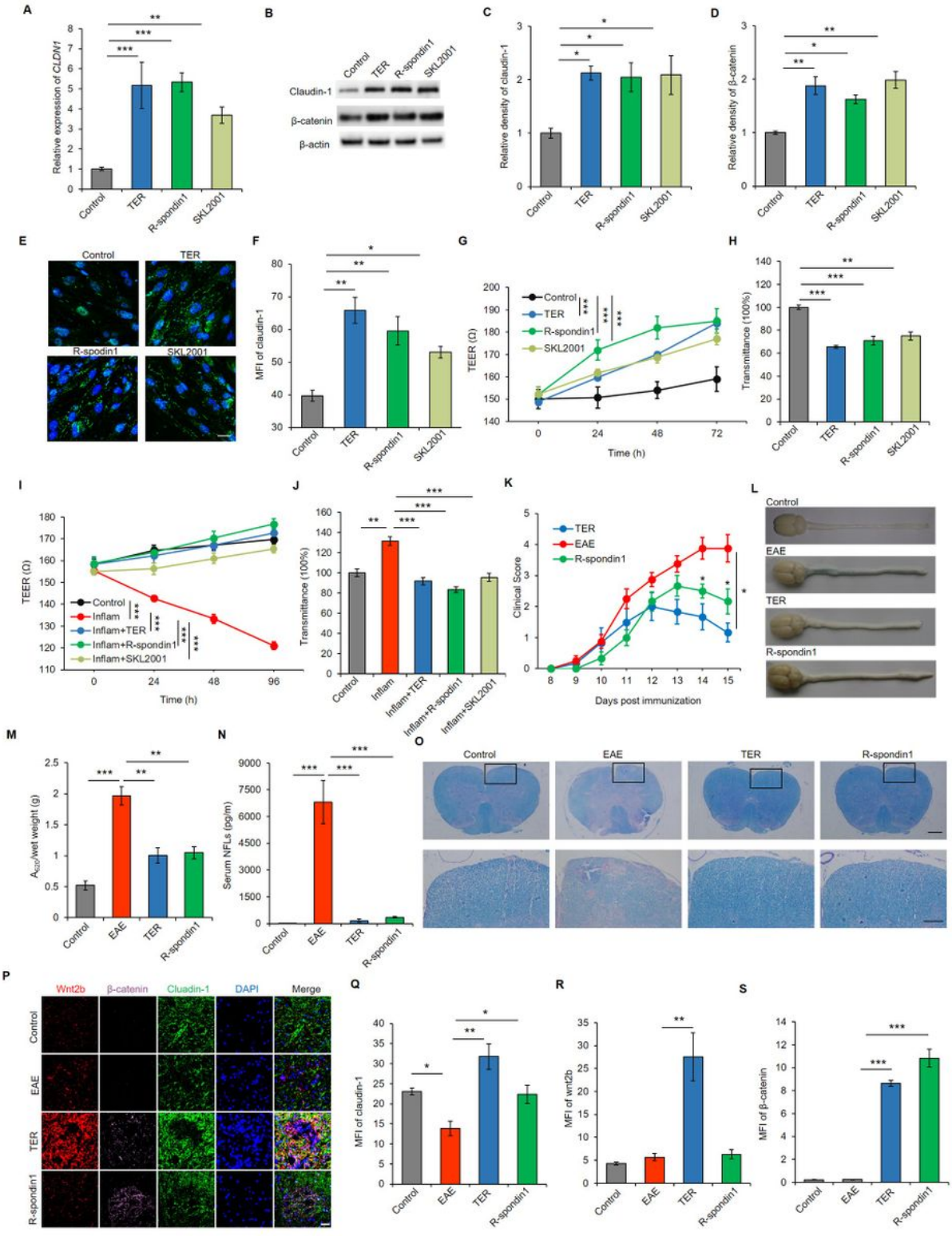

Figure 7

The activation of Wnt singaling promoted claudin-1 expression and protected BBB integrity in EAE model. (**A**) Gene expressions of *CLDN1* determined by quantitative PCR. Error bars represent ± s.e.m. (n = 3). (**B**) Western blot images and quantitative analysis of (**C**) claudin-1 and (**D**) β-catenin in HBMECs. Error bars represent ± s.e.m. (n = 3). (**E**) Confocal images and (**F**) quantitative analysis of claudin-1 in HBMECs. Scale bar: 20 μm. Error bars represent ± s.e.m. (n = 3). (**G**) The TEER of HBMECs BBB model over 3 d with TER and Wnt agonists and (**H**) transmittance of NAF after the experiment. Error bars represent ± s.e.m. (n = 3). (**I**) The TEER of inflammatory injury BBB model over 3 d with Wnt agonists treatment and (**J**) transmittance of NAF after the experiment. Error bars represent ± s.e.m. (n = 3). (**K**) Clinical scores of EAE rats with TER and Wnt agonist treatment. Error bars represent ± s.e.m. (n = 6). (**L**) Extravasation of Evans blue into the CNS 24 h after intravenous injection and (**M**) quantification analysis. Error bars represent ± s.e.m. (n = 3). (**N**) Detection of NFLs in the rat serum after the experiments. Error bars represent ± s.e.m. (n = 3). (**O**) The LFB staining of spinal cords in each group. Scale bar: upper 200 μm, below 40 μm. (**P**)The immunofluorescence images and quantitative analysis of (**Q**) claudin-1, (**R**) Wnt2b and (**S**) occludin in the spinal cords. Scale bar: 20 μm. Error bars represent ± s.e.m. (n = 3). Statistical significance of clinical scores was analyzed by the generalized equation, and others were assessed by ANOVA with Newman-Keuls test. *p 0.05, **p 0.01, ***p 0.001.

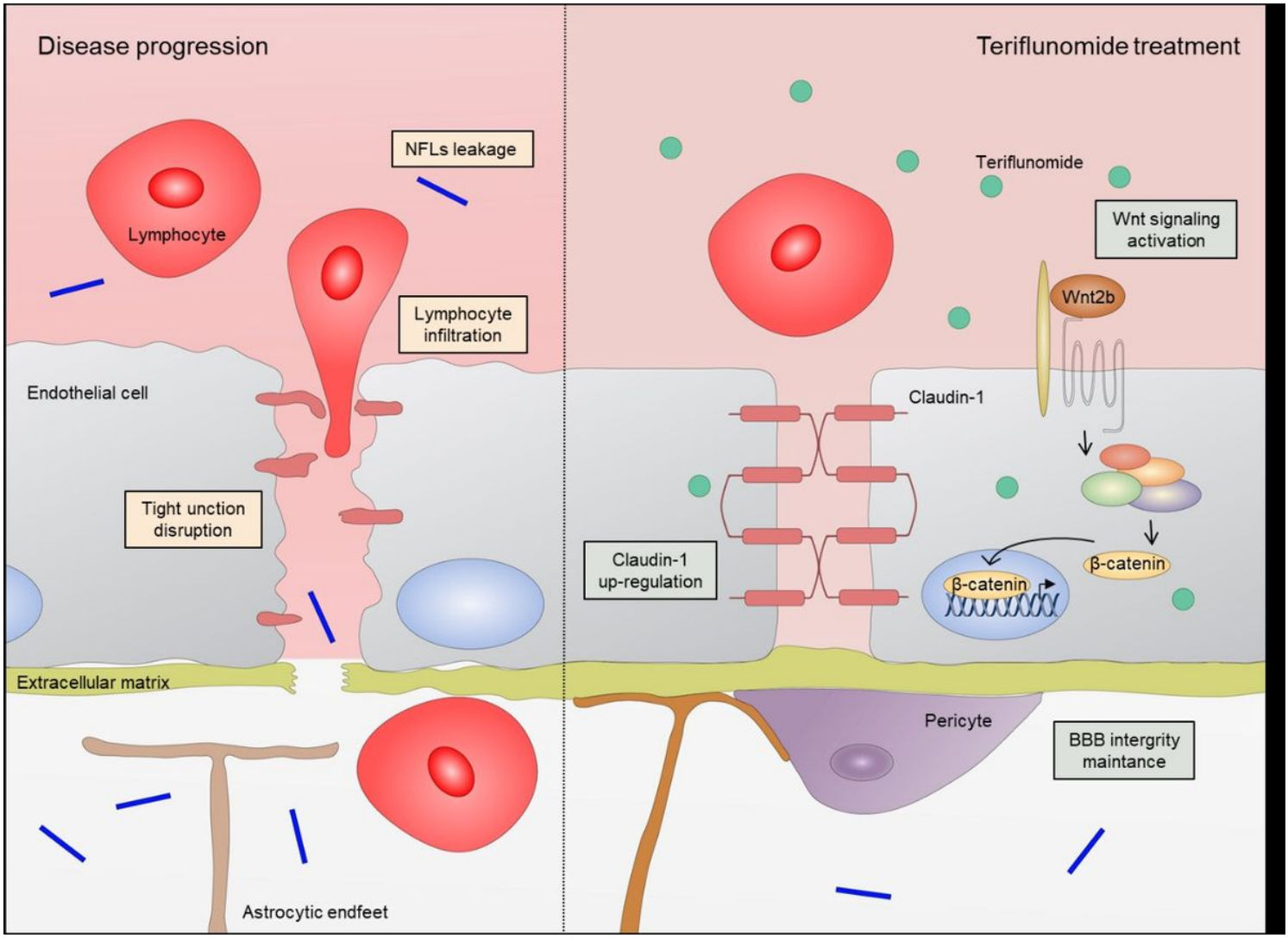

Figure 8

Schematic for teriflunomide-mediated novel mechanism of BBB protection in MS. The breakdown of BBB and tight junction disruption led to peripheral lymphocyte infiltration and CNS NFLs leakages in MS. Teriflunomide promoted tight junction protein claudin-1 expression through Wnt signaling activation, thereby ameliorating BBB injuries.

Supplementary Files

This is a list of supplementary files associated with this preprint. Click to download.

- Fig.S1.jpg
- Fig.S2.jpg
- Fig.S3.jpg
- Fig.S4.jpg
- Fig.S5.jpg